- Technical Paper -

GEOMETRIC PARAMETERS RELATING CORROSION PENETRATION TO SURFACE CRACK WIDTH

Di QIAO[*1], Hikaru NAKAMURA[*2], Yoshihito YAMAMOTO[*3] and Taito MIURA[*4]

ABSTRACT

This study aims to clarify the decisive geometric parameters relating corrosion penetration to surface crack width. The corrosion-induced crack propagation was simulated using the Rigid Body Spring Method considering varying geometric parameters of concrete sections, and regression analysis of the simulation results was performed. It was found that the deformation area of concrete surface has a great influence on surface cracking. For a certain type of concrete material, the critical corrosion penetration producing visible surface crack can be expressed in a linear form in terms of the cover-to-bar diameter ratio and the width of surface deformation area. On the other hand, the growth rate of crack width is linearly proportional to the ratio of cover to the width of surface deformation area.

Keywords: corrosion penetration, surface crack width, surface deformation area, RBSM

1. INTRODUCTION

Corrosion of reinforcing steel bars is a principal cause of deterioration of reinforced concrete (RC) structures. The volume expansion of forming corrosion products causes concrete cracking, which affects the serviceability of a RC structure. On the other hand, the cross-section loss of a reinforcing bar due to a high level of corrosion may have a great influence on the structural performance. Understanding of the relationship between corrosion penetration (nominal radius loss due to corrosion) and surface crack width can not only help predict crack development contributing to efficient maintenance work, but also be useful for assessing the state of corrosion using crack width from visual inspection [1, 2].

A number of models relating corrosion amount to surface crack width have been proposed [1, 2, 3, 4]. The method used to develop such models can be divided into two groups: statistical analysis of test data and mechanistic-based modeling. The research group directed by François in France conducted long-term corrosion tests on RC beams (up to 26 years), and attempted to link surface crack width with steel cross-section loss [1, 4]. Their results showed that the empirical models derived with regression analysis of test data strongly depends on the type of the specimens tested and environmental conditions. For limited test data used to derive empirical models, the applicability of these models is usually limited. Mechanistic-based modeling, however, can be adopted for considering a great number of parameters relating to the geometric properties and concrete material properties. Chernin et al. [2] examined the influence of the geometry of a concrete section using finite element modeling, but they used a polynomial series in terms of concrete cover, bar diameter and side cover for deriving formulae relating corrosion penetration to surface crack width. The parameters that play key roles on surface crack development are not clear.

The purpose of the study is to clarify the decisive parameters relating corrosion penetration to surface crack width using numerical modeling, which can offer guidelines for deriving formulae with test data in the future. The present paper focuses on the influence of variation of several parameters concerning geometric properties, including concrete cover thickness, section width, bar diameter and the location of a reinforcing bar. In the numerical study, the Rigid Body Spring Method (RBSM) with the corrosion-expansion model [5] was used to investigate the development of surface crack width caused by corrosion.

2. NUMERICAL ANALYSIS OF CORROSION-INDUCED CONCRETE CRACKING

2.1 Three-dimensional RBSM

In the analysis, three-dimensional RBSM was employed [6]. The RBSM as a discrete numerical approach represents a continuum material as an assemblage of rigid particles interconnected by zero-length springs along their boundaries as shown in Fig.1. The particle elements are randomly generated with Voronoi Diagram. Each of the elements has six degrees of freedom at its nucleus. Three springs, one normal and two shear springs, are defined at the center point of each triangle formed by the center of gravity and the vertices of the boundary between two elements.

*1 Postdoctoral Fellow, Dept. of Civil Engineering, Nagoya University, Dr.E., JCI Member
*2 Professor, Dept. of Civil Engineering, Nagoya University, Dr.E., JCI Member
*3 Associate Prof., Dept. of Civil Engineering, Nagoya University, Dr.E., JCI Member
*4 Assistant Prof., Dept. of Civil Engineering, Nagoya University, Dr.E., JCI Member

Nonlinear material models of concrete were introduced into the springs. The response of the spring model provides an understanding of the interaction between particles instead of the internal behavior of each element based on continuum mechanics.

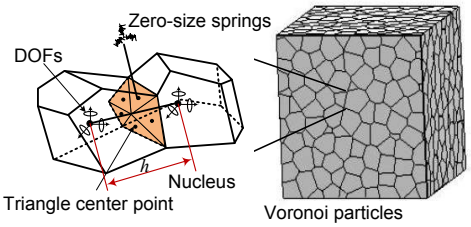

Fig.1 Voronoi particle definition of RBSM element

2.2 Corrosion-expansion model [5]

The volume expansion of corrosion products is modeled by internal expansion pressure, as shown in Fig.2. A three-phase material model consisting of steel bar, corrosion products and concrete is created. The steel bar and corrosion products layer are both modeled as elastic materials, and the thickness of the corrosion products layer H is assumed to be constant. The former work showed that when the thickness H is set as 1.0mm and the Young's modulus of corrosion products is assumed as 500MPa, the model simulates reasonable cracking behavior compared with the electric corrosion test results. These assumptions have been adopted in this study.

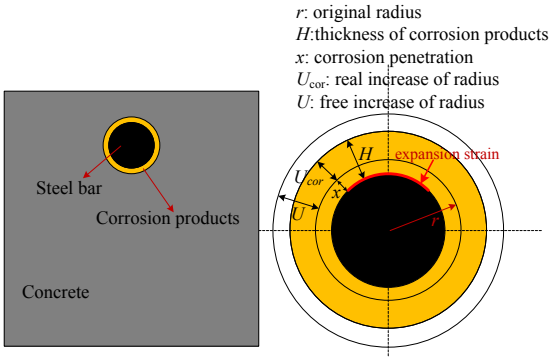

Fig.2 Corrosion-expansion model

The internal expansion pressure is dealt with the initial strain problem with increment of initial strain $\Delta\varepsilon_0$ ($\Delta\varepsilon_0=\Delta U/H$) in each analysis step. In this study, general corrosion along the steel bar length was assumed. The accumulative free increase of bar radius U as input data can be determined by corrosion penetration x:

$$U = (\alpha_{cor} - 1)x = (\alpha_{cor} - 1)r\Delta m/2m \qquad (1)$$

Where,

α_{cor} : volume-expansion ratio of corrosion products, which was assumed to be 2.5
r : original bar radius
Δm : mass loss of steel bar due to corrosion
m : original mass of steel bar

The results of the electric corrosion tests conducted previously [7] showed that the steel bars were corroded much more in a part surrounded by cracked concrete. In order to take account of the influence of forming cracks on the corrosion process, a non-uniform corrosion model [5] was employed as shown in Fig.3. The localized corrosion after crack initiation is assumed that the corrosion products are only distributed over one quarter of the steel bar circumference when a vertical crack with a width greater than 0.1mm appears in the concrete cover. The increment of initial strain is thus applied only to one quarter of the model, while the total mass loss is the same as that in the uniform corrosion model.

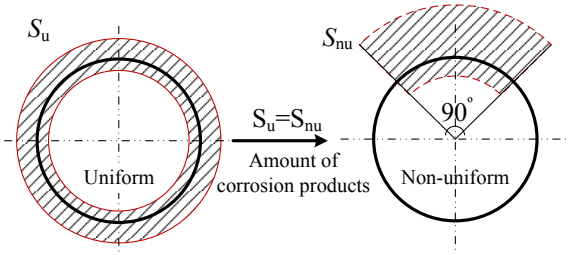

Fig.3 Assumed corrosion process

It has been indicated that a part of corrosion products penetrate into concrete cracks, and do not contribute to the expansion pressure causing concrete cracks [8]. The present study, however, did not take into consideration this effect, since a maximum of 0.3mm crack width relating to the service limit state [9] was considered. Under such a situation the penetration of corrosion products may be insignificant. This assumption is supported by the former test result that the speed of surface crack propagation slows after the crack width reaches 0.4mm [7].

2.3 Analysis outline

The specimens analyzed had a length of 100mm and a height of 200mm, each containing a single steel bar. Two series with different locations of a steel bar in a concrete section, center located and corner located, were considered, as shown in Fig.4. A large number of parameters relating to the geometry, such as cover thickness c, bar diameter d, side cover thickness s and s_l, and section width W, were examined. They are summarized in Table 1.

Fig.5 shows an example of the RBSM models created with Voronoi Diagram. The size of the particle elements near the steel bar is 2mm, while the mesh size for the outer part is 30mm.

Table 1 Summary of analytical parameters for concrete sections

Series	Cover c (mm)	Bar diameter d (mm)	Section width W (mm)	
Center located	10, 30, 50	10, 16, 22	50, 150, 300, 500	
Corner located	30	16	Cover s (mm)	Cover s_l (mm)
			50, 100	100, 150, 200, 250,300

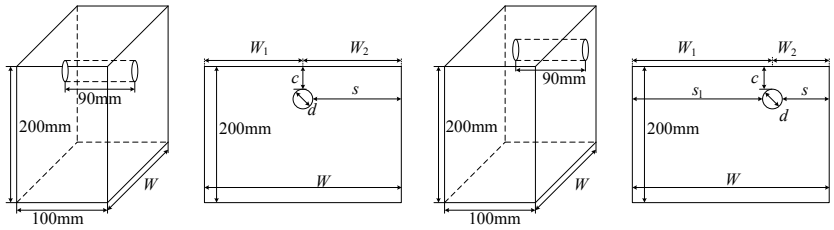

(a) Center located (b) Corner located

Fig.4 Specimen dimensions

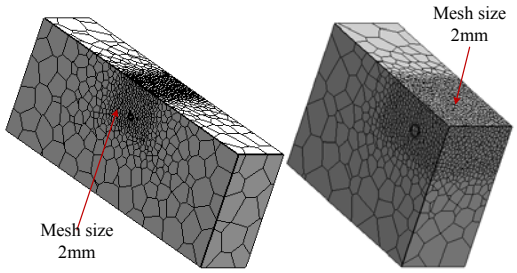

Fig.5 3D view of RBSM models

In the analysis, the tensile and compressive strengths of the concrete simulated were 2.5MPa and 39.0MPa respectively, which was confirmed by tension and compression simulations of a standard cylinder with a mesh size of 2mm.

3. ANALYSIS OF RESULTS

3.1 Crack patterns

The crack patterns are strongly related to the geometry of the concrete section. Fig.6 shows three types of crack patterns found for the series with a center located rebar, corresponding to a corrosion penetration of 160μm. For $c/s > 1$, there is no vertical crack above the steel bar, and delamination occurs (Type I). For $c/s < 1$ and $c/d \leq 1$, if the section width is relatively large ($W \geq 150$mm), an inclined lateral crack appears in the concrete cover besides the vertical crack, and multi-cracks appear on the concrete surface (Type II). For $c/s < 1$ and $c/d > 1$, a vertical crack together with two lateral cracks occur (Type III). The analysis of surface crack evolution was performed on the specimens satisfying $c/s < 1$ and $c/d > 1$, since they all yield a single longitudinal crack on the top surface of concrete.

3.2 Development of surface crack width

Fig.7 presents surface crack width against corrosion penetration for different simulation cases. The crack initiation represents the occurrence of a visible crack wider than 0.05mm [9]. After that, the crack width increases nearly linearly as corrosion penetration increases, because the penetration of corrosion products into concrete cracks was not considered in the present study. It is obvious that, for the same section width, the surface crack initiation is delayed with an increase of cover-to-bar diameter ratio (c/d). On the other hand, the growth of surface crack width becomes slower when the section width is larger. These results indicate a clear influence of the geometry of concrete sections on the development of surface crack width.

For deriving formulae relating corrosion penetration to surface crack width, the connection between geometric parameters and the critical corrosion penetration x_i (μm) triggering surface cracking as well as the increasing rate of crack width β was investigated in detail. The calculation of β refers to the model proposed by Rodriguez et al. [3], as explained in Eq.2 and Fig.8. The width of surface crack up to 0.3mm was considered for calculating β.

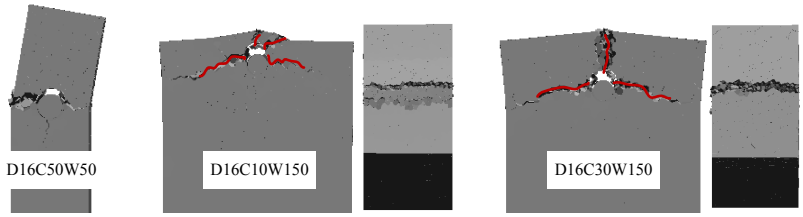

(a) Type I (b) Type II (c) Type III

Fig.6 Different crack patterns related to c/s and c/d (magnification× 20)

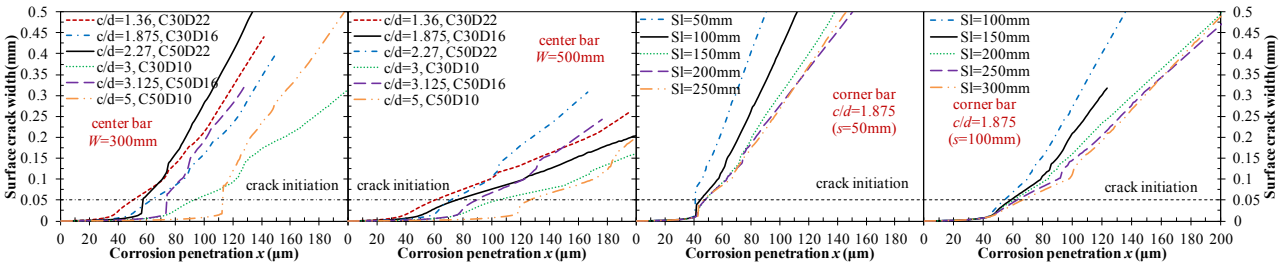

Fig.7 Surface crack development for different specimens

$$w = 0.05 + \beta(x - x_i) \quad (2)$$

Where,

w : surface crack width (mm) induced by a corrosion penetration x (μm)

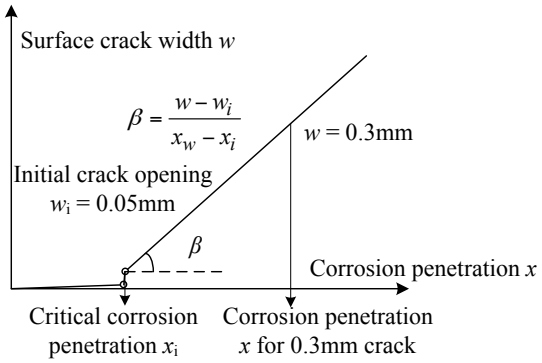

Fig.8 Model for development of surface crack width

3.3 Critical corrosion penetration for crack initiation

Fig.9 depicts the critical corrosion penetration x_i for the specimens with different ratios of cover-to-bar diameter c/d. Linear relationships between x_i and c/d can be found for varying section widths with the coefficient of determination larger than 0.85. This is in agreement with the findings by Rodriguez et al. [3] and Alonso et al. [10] derived from the electric corrosion test results. In addition, it seems that as the section width W increases, the critical corrosion penetration also rises. Kawamura et al. [7] measured the concrete surface deformation resulting from the expansion of corrosion products after the electric corrosion test. Their data suggested that surface crack development is closely related to the concrete surface deformation. Then the surface area actually contributing to surface cracking (effective deformation area) was examined.

Fig.10 shows the concrete surface deformation when a visible crack appears on the concrete surface. As can be seen, at this stage only a part of concrete surface is elevated. The relationship between critical corrosion penetration x_i and the width of effective deformation area W_{ei} at crack initiation is evaluated as shown in Fig.11. There is also a linear relationship between x_i and W_{ei}.

Generally, for the concrete with similar strength and porosity, x_i can be calculated as:

$$x_i = a_{c/d}(c/d) + a_{W_{ei}} W_{ei} + k \quad (3)$$

Where,

$a_{c/d}$, a_{Wei}, k: coefficients

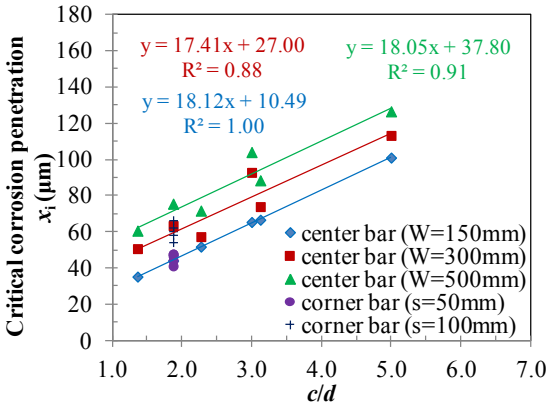

Fig.9 Relationship between x_i and c/d

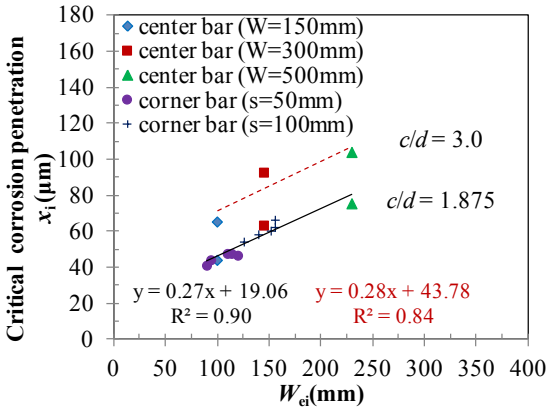

Fig.11 Relationship between x_i and W_{ei}

3.4 Relationship between surface crack width and corrosion penetration

Fig.12 shows the deformation of concrete surface when the surface crack width reaches 0.2mm. Comparing Fig.10 and Fig.12, it can be found that, as surface crack propagates, the deformation area becomes larger. On the other hand, for both stages, it appears that the parameter c/d has no appreciable effect on the effective deformation area, and the width of the deformation area may be constant for a given section width (see the series with a center located bar). These two values for different specimen dimensions are compared in Fig.13. Since the series with a corner bar showed an asymmetric deformation pattern, the area is divided into two sides denoted by W_{e1} and W_{e2} for comparison (see Fig.10 and Fig.12). Based on regression analysis, it was found that within the section dimension investigated the relation between W and W_e at each side of the steel bar could be described using the same power trend line. The coefficients for the power relationship, a_W and b, depend on the surface cracking

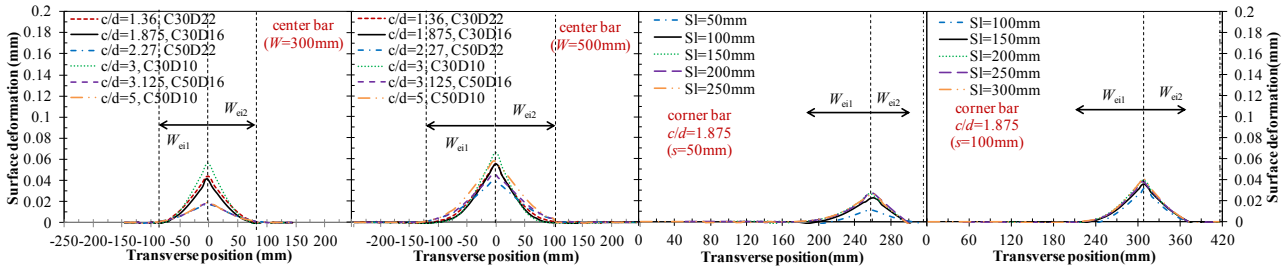

Fig.10 Surface deformation at surface crack initiation

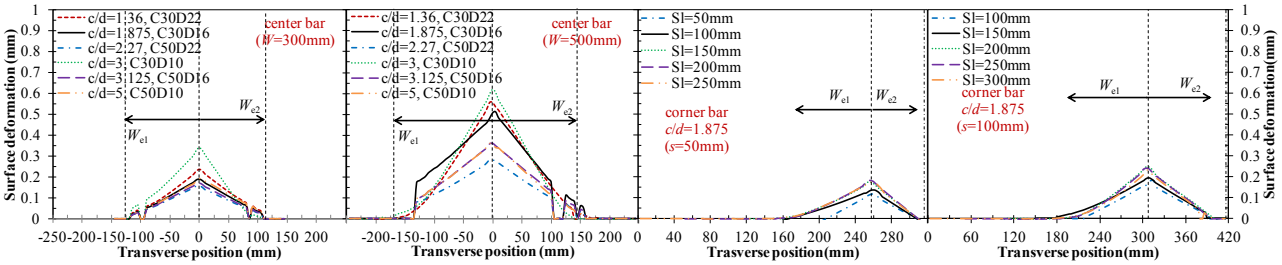

Fig.12 Surface deformation with crack width reaching 0.2mm

state. The width of the effective deformation area can thus be determined as:

$$W_e = a_W W_1^b + a_W W_2^b \quad (4)$$

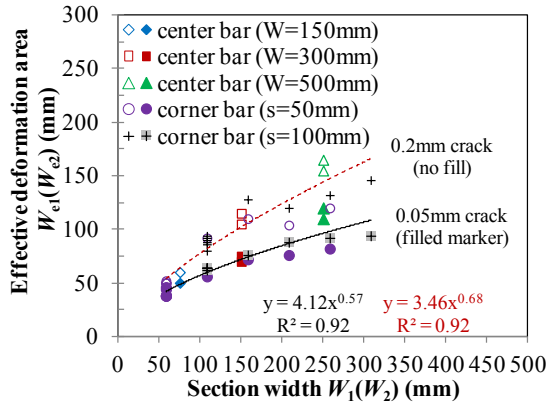

Fig.13 Relationship between $W_1(W_2)$ and $W_{e1}(W_{e2})$

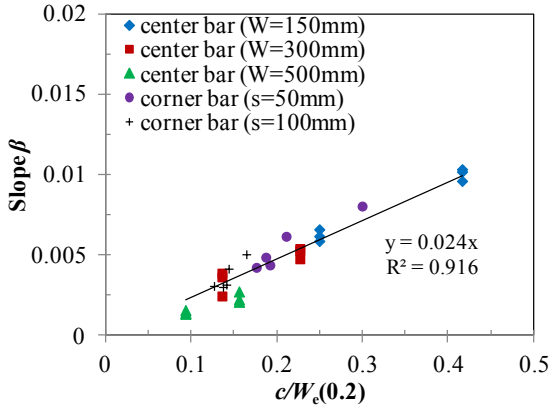

Fig.14 Relationship between β and c/W_e

In order to determine the crack growth rate β, we examined several parameters such as c/d, c/s, W_e, etc. for their connections with β, in which W_e corresponds to a surface crack width of 0.2mm. It was found that β is in proportion to the c/W_e ratio, as shown in Fig.14:

$$\beta = a_{c/W_e}(c/W_e) \quad (5)$$

Where,

$a_{c/We}$: coefficient

Vidal et al. [1] and Rodriguez et al. [3] both suggested a constant value for β on the basis of test data, while in this study it shows that β may be influenced by concrete cover and the section width. A comparison between the derived formulae and the empirical model by Vidal et al. [1] is performed using available test data in the next part.

3.5 Comparison of derived formulae with test data

Fig.15 shows the comparison of the derived formulae and the empirical model with the test data obtained by Kawamura et al. [7]. In their test, a great number of RC specimens with a single center located bar and different geometric conditions were tested using the impressed current method. The coefficients for our formulae were determined by regression analysis on the simulation results as presented earlier:

$$W_{ei} = 4.12W_1^{0.57} + 4.12W_2^{0.57} \quad (6)$$

$$x_i = 17.86(c/d) + 0.27W_{ei} - 14.43 \quad (7)$$

$$W_e = 3.46W_1^{0.68} + 3.46W_2^{0.68} \quad (8)$$

$$w = 0.05 + 0.024(c/W_e)(x - x_i) \quad (9)$$

It should be noted that a rigorous approach for determination of relevant coefficients should involve the use of a significant amount of laboratory test data and field measurements.

Vidal et al. [1] developed their model based on the results of long-term natural corrosion, which is expressed as:

$$w = 0.0575(\Delta A_s - \Delta A_{s0}) \quad (10)$$

$$\Delta A_s = \pi x(2r - x) \quad (11)$$

$$\Delta A_{s0} = \pi r^2\left[1 - \left[1 - \frac{2}{d}\left(7.53 + 9.32\frac{c}{d}\right)10^{-3}\right]^2\right] \quad (12)$$

Where,

ΔA_s : cross-section loss of steel bar

ΔA_{s0} : cross-section loss for crack initiation

From Fig.15 it can be seen that both models, the derived formulae and the model by Vidal et al., show an earlier surface crack initiation than the test data, especially for the case with a concrete cover of 45mm. One possible reason for the discrepancy between the formulae and the test data is the disregard of the influence of varying concrete porosity. High concrete porosity may result in more corrosion products accommodated in concrete pores, delaying the initiation of corrosion-induced cracks. After crack initiation, the derived formulae, however, predict well the increasing rate of crack width β up to a crack width of 0.4mm. Moreover, the formulae can capture the varying trend of β resulting from varied concrete section width, i.e. the cracking speed is slower for a wider concrete section. On the other hand, the empirical model by

Vidal et al. [1] cannot describe the influence of section width on surface crack propagation because of the limited test data they used to relate the crack width with cross-section loss (limited geometric properties of the specimens tested). This result indicates that the parameters relating to the section geometry, c/d, W_{ei} and c/W_e, should be considered for linking corrosion penetration with surface crack width.

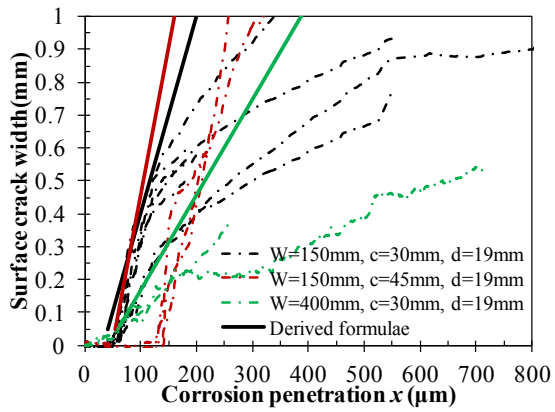

(a) Derived formulae

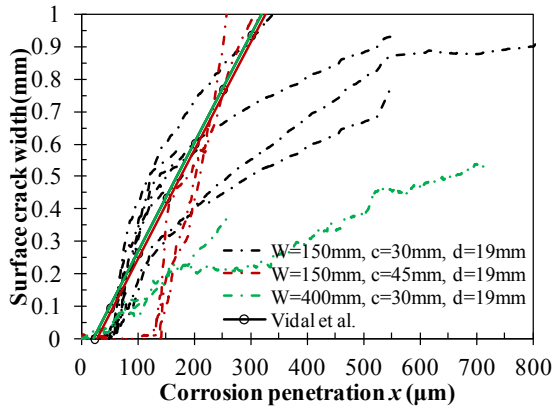

(b) Model by Vidal et al.

Fig.15 Comparison of models with test data

4. CONCLUSIONS

This study examined the surface crack development of RC specimens with various geometric parameters resulting from corrosion of a steel bar. Regression analysis was performed to determine the decisive parameters relating corrosion penetration to crack width. The following conclusions can be derived from the present study:

(1) The effective deformation area of concrete surface may affect both surface crack initiation and the development of crack width. The width of the deformation area can be determined using a power relation considering the section width at both sides of a steel bar.

(2) For a certain concrete material, the critical corrosion penetration for surface crack initiation is in linear relationship with the c/d ratio and the width of the surface deformation area W_e.

(3) The increasing rate of crack width, determined as the slope between initial visible crack and 0.3mm wide crack, is proportional to the c/W_e ratio.

In the present study, the formulae were obtained only considering the influence of the geometry. The other factors, such as local distribution of corrosion along a steel bar and penetration of corrosion products into pores and cracks, may have a great influence on crack evolution. Further numerical study is needed.

ACKNOWLEDGEMENT

This work was supported by Council for Science, Technology and Innovation, "Cross-ministerial Strategic Innovation Promotion Program (SIP), Infrastructure Maintenance, Renovation, and Management" (funding agency: NEDO). The authors also acknowledge the supports of Grants-in-Aid for Scientific Research B (15H04033).

REFERENCES

[1] Vidal, T., Castel, A. and François, R., "Analyzing Crack Width to Predict Corrosion in Reinforced Concrete," Cem. & Conr. Res., Vol. 34, 2004, pp. 165-174.

[2] Chernin, L., Stewart, M. G. and Val, D. V., "Prediction of Cover Crack Propagation in RC Structures Caused by Corrosion," Mag. Conr. Res., Vol. 64(2), 2012, pp. 95-111.

[3] Rodriguez, J. et al., "Corrosion of reinforcement and service life of concrete structures," Proc. 7th International Conference on Durability of Building Materials and Components, (Sjöstrmöm, C. (ed.)), E & FN Spon, London, Vol.1, 1996, pp. 117-126.

[4] Khan, I., François, R. and Castel, A., "Prediction of Reinforcement Corrosion Using Corrosion Induced Cracks Width in Corroded Reinforced Concrete Beams," Cem. & Conr. Res., Vol. 56, 2014, pp. 84-96.

[5] Tran, K. K. et al., "Analysis of Crack Propagation due to Rebar Corrosion Using RBSM," Cem. Conr. Compos., Vol. 33, 2011, pp. 906-917.

[6] Yamamoto, Y. et al., "Analysis of Compression Failure of Concrete by Three-dimensional Rigid Body Spring Model," Doboku Gakkai Ronbunshuu, JSCE, Vol. 64, 2008, pp.612-630. (in Japanese)

[7] Kawamura, K. et al., "Concrete Surface and Internal Cracks Propagation due to Rebar Corrosion," Proc. JCI, Vol. 32, 2010, pp. 1007-1012. (in Japanese)

[8] Wong, H. S. et al., "On the Penetration of Corrosion Products from Reinforcing Steel into Concrete due to Chloride-induced Corrosion," Corros. Sci., Vol. 52(7), 2010, pp. 2469-2480.

[9] Andrade, C., Alonso, C. and Molina, F. J., "Cover Cracking as a Function of Bar Corrosion: Part I – Experimental test," Mater. Struct., Vol. 31, 1993, pp. 453-464.

[10] Alonso, C. et al., "Factors Controlling Cracking of Concrete Affected by Reinforcement Corrosion," Mater. Struct., Vol. 31, 1998, pp. 435-441.